PU/NU-03-17

U. S. Department of Energy
Nuclear Engineering Education Research

ANALYTICAL AND EXPERIMENTAL STUDY OF THE EFFECTS OF NON-CONDENSABLE IN A PASSIVE CONDENSER SYSTEM FOR THE ADVANCED BOILING WATER REACTOR

Project Carried Out With Support From US DOE Under Award NO: DE-FG07-00ID13928

Final Report

S. T. Revankar, S. Oh

PURDUE UNIVERSITY

SCHOOL OF NUCLEAR ENGINEERING

PU/NU-03-17

U. S. Department of Energy
Nuclear Engineering Education Research

ANALYTICAL AND EXPERIMENTAL STUDY OF THE EFFECTS OF NON-CONDENSABLE IN A PASSIVE CONDENSER SYSTEM FOR THE ADVANCED BOILING WATER REACTOR

Final Report
May, 2000 to July, 2003

DOE Project DE-FG07-00ID13928

Principal Investigator:
Shripad T. Revankar
Purdue University
School of Nuclear Engineering
West Lafayette, IN 47906-1290
765-496-1782
shripad@ecn.purdue.edu

Contributing Authors:

S. T. Revankar*, and S. Oh

Purdue University
School of Nuclear Engineering
West Lafayette, IN 47906-1290

September 2003

* Project Director

CONTENTS

LIST OF FIGURES

LIST OF TABLES

ACRONYMS

DP	Differential Pressure
DW	Dry Well
HTC	Heat Transfer Coefficient
NRC	Nuclear Regulatory Commission
PCCS	Passive Containment Cooling System
SBWR	Simplified Boiling Water Reactor
SP	Suppression Pool
UCB	University of California Berkeley

NOMENCLATURE

C_p	Specific heat [j/kg·C]
d	Diameter [m]
g	Gravitational acceleration [m/s^2]
h	Heat transfer coefficient[W/m^2·C] or Enthalpy [J/kg]
h_{fg}	Latent heat of vaporization [J/kg]
Ja	Jakob Number
k	Conductivity [W/m^2·C]
m	Mass flow rate [kg/s]
M	Molecular weight [g/mol]
Nu	Nusselt Number
P, p	Pressure [Pa]
q''	Heat flux [W/m^2]
Q	Heat Transfer Rate [W]
Re	Reynolds number
T	Temperature [K or C]
V	Average velocity [m/s]
W	Mass fraction

Greek Symbols

δ	Film thickness [m]
μ	Dynamic viscosity [kg/m·s]
ρ	Density [kg/m^3]
Γ	Mass flow rate per unit length [kg/m·s]

Subscripts

a	Air
bulk	Bulk
G	Steam-gas mixture
I	Interface
L	Liquid
SAT	Saturation
TOT	Total
v	Vapor
W	Wall

1. PROJECT SUMMARY

The main goal of the project is to study analytically and experimentally condensation heat transfer for the passive condenser system relevant to the safety of next generation nuclear reactor such as Simplified Boiling Water Reactor (SBWR). The objectives of this three-year research project are to: 1) obtain experimental data on the phenomenon of condensation of steam in a vertical tube in the presence of non-condensable for flow conditions of PCCS, 2) develop a analytic model for the condensation phenomena in the presence of non-condensable gas for the vertical tube, and 3) assess the RELAP5 computer code against the experimental data. The project involves experiment, theoretical modeling and a thermal-hydraulic code assessment. It involves graduate and undergraduate students' participation providing them with exposure and training in advanced reactor concepts and safety systems.

In this final report, main tasks performed during the project period are summarized and the selected results are presented. Detailed descriptions for the tasks and the results are presented in each yearly report (Refs. 1~3).

2. EXPERIMENTAL PROGRAM

2.1 Scaling Analysis

A detailed scaling analysis for the PCCS condenser was performed. The scaling parameters were identified to scale down the prototype condenser design. The effect of the non-condensable in the scaled condenser was discussed and its implication on the scaled test facility was presented.

2.2 Test Facility Design

An experimental loop was designed with 5.08 cm diameter condenser for forced flow cooling and 2.54 cm diameter condenser for pool boiling cooling. The design of the condenser tube was based on the scaling analysis. The test section and the loop were instrumented for required parameters.

2.3 Test Results

Results for 5.08 cm diameter condenser for forced flow cooling are presented in Ref. 2. In this section, selected results for 2.54 cm diameter condenser for pool boiling cooling mode are presented.

Condensation experiments were performed for three PCCS operation modes, i.e., 1) Through flow mode, 2) Periodic venting mode, and 3) Complete condensation mode. The complete condensation mode was performed for the pure steam condition varying the inlet steam flow rate. For a given steam flow rate in this mode, the system pressure is uniquely determined by the heat removal capacity of the condenser. The periodic venting mode was initiated from the complete condensation mode by putting small amount of air. Through flow mode was performed varying the inlet steam flow rate, inlet air flow rate, and system pressure.

1) Complete Condensation Mode

Fig. 2.1 shows the condensation heat transfer rate with the system pressure. Fig. 2.2 shows the various heat transfer coefficients (HTC) for the complete condensation mode with system pressure. The overall HTC remains almost constant and condensation HTC decreases with increase of system pressure.

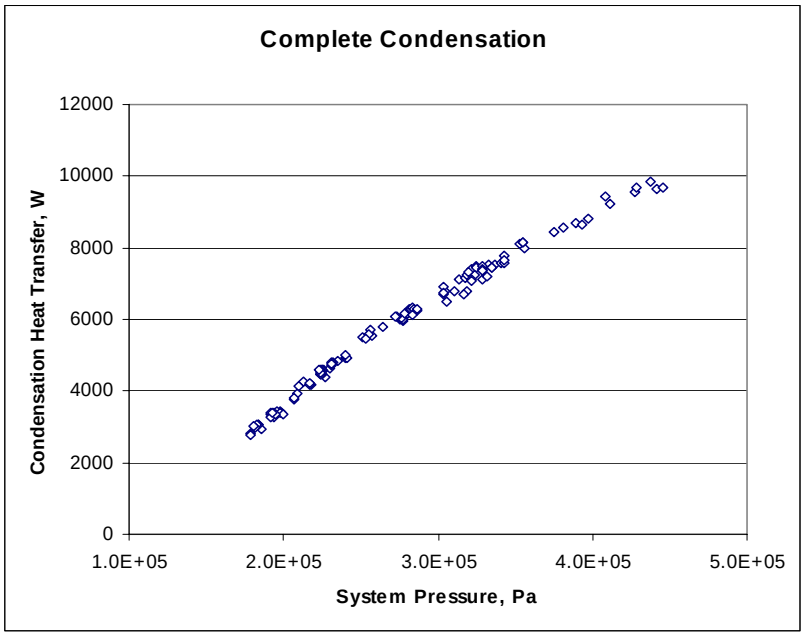

Figure 2.1 Complete Condensation: Condensation Heat Transfer Rate

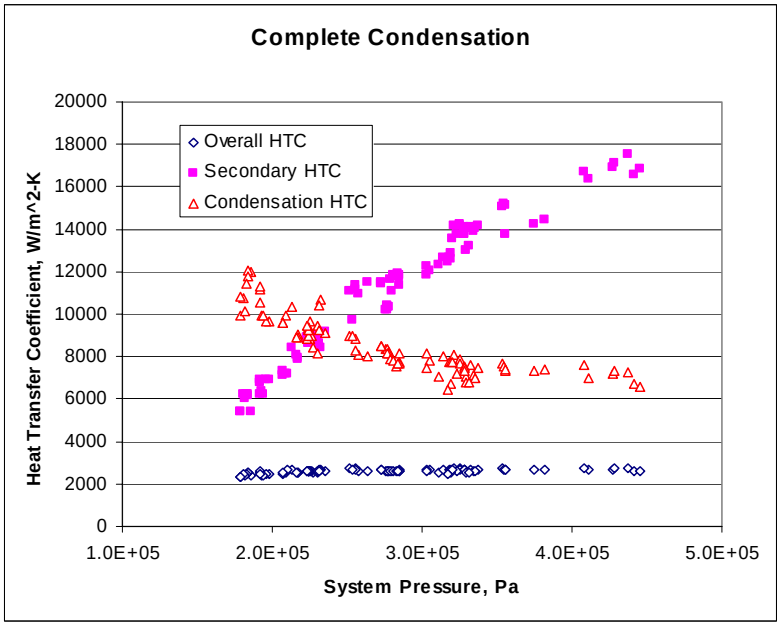

Figure 2.2 Complete Condensation: Heat Transfer Coefficients

2) Through Flow Mode

Pure Steam Data as a Function of Pressure

Fig. 2.3 shows the effect of system pressure for pure steam condition (inlet steam flow rate = 4.96 g/s) for through flow mode. Overall HTC is almost constant with system pressure. Secondary HTC increases with system pressure and condensation HTC decreases with system pressure. This trend is very similar to the results of complete condensation mode.

Effect of Noncondensable Gas

Fig. 2.4 shows the Effects of noncondensable gas mass fraction for P=0.28 MPa, Msteam=3.6 g/s. As shown in this figure, the noncondensable gas degrades the performance of the condensation.

Effect of Steam Flow Rate

Fig. 2.5 shows the effects of noncondensable gas mass fraction and steam flow rate for P=0.34 MPa. From this figure, the condensation performance and condensation HTC increase with inlet steam flow rate.

Effect of System Pressure

Fig. 2.6 shows the effects of system pressure at Msteam=2.5 g/s, Wair=0.2% condition. The condensation HTC decreases with system pressure.

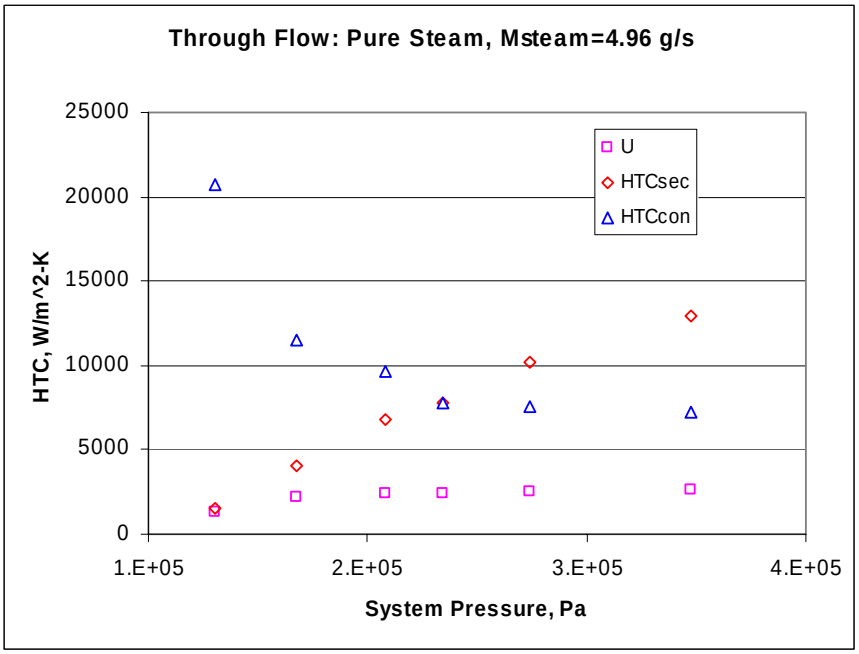

Figure 2.3 Through Flow: Heat Transfer Coefficient for Pure Steam

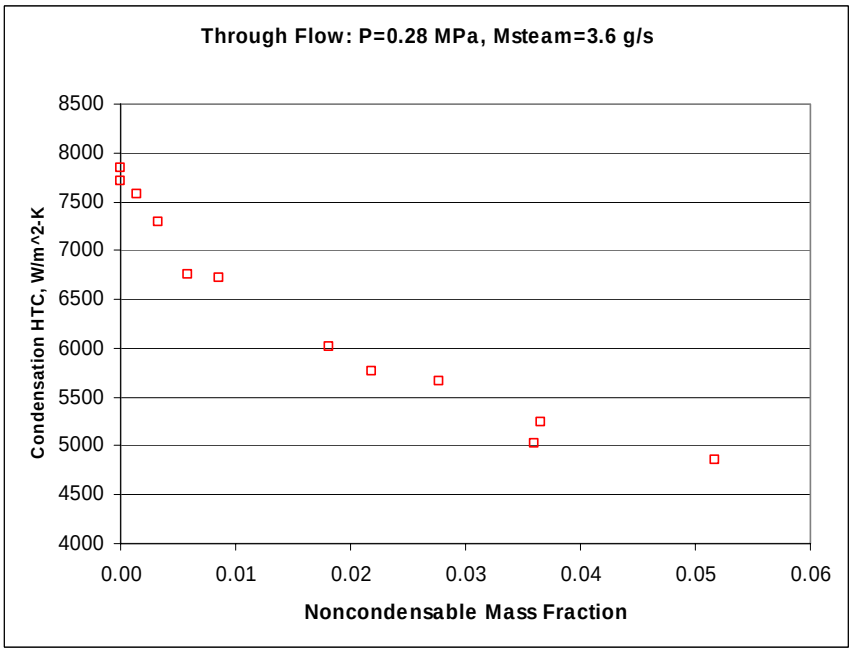

Figure 2.4 Through Flow: Condensation HTC at P=0.28 MPa, Msteam=3.6 g/s

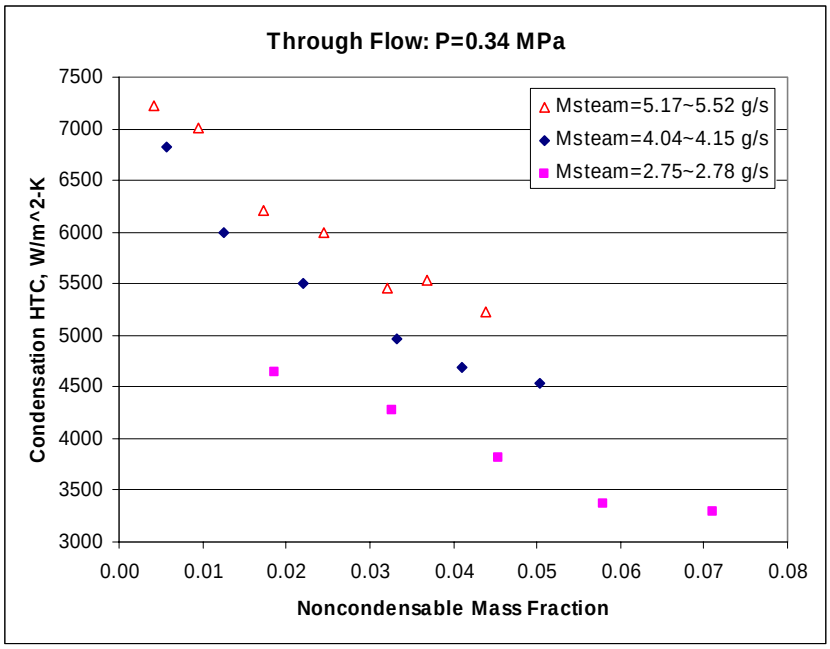

Figure 2.5 Through Flow: Condensation HTC at P=0.34 MPa

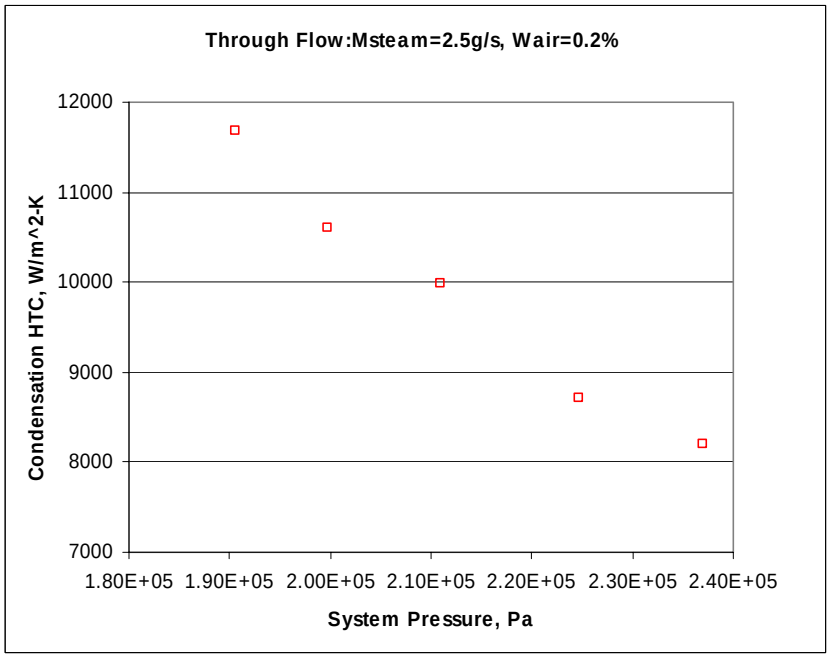

Figure 2.6 Through Flow: Condensation HTC at Msteam=2.5 g/s, Wair=0.2%

3) Periodic Venting Mode

Periodic venting mode is initiated from the Complete Condensation Mode by putting small amount of air. As the noncondensable air is accumulating in the system, the condensation

performance is degraded and this lead to the increase of the system pressure. Besides this effect, adding the air itself also increases the system pressure. For the prototype SBWR, the PCCS vent line is submerged in the SP with 800mm depth from the SP water surface. It corresponds to approximately 1 psi hydrostatic head. If the drywell pressure is greater than the SP pressure by this amount of the hydrostatic head, the noncondensable gas and uncondensed steam in the PCCS will be vented to the SP. During the venting, the noncondensable gas in the PCCS is cleared and the DW pressure decreases. After the venting, the pressurization in the DW resumes and this cycle repeats. Our test facility is designed for ½ height scaling, the head due to submergence of the vent line (DPvent) in the SP is 0.5 psi. So, when the pressure increases about 0.5 psi from the base pressure, the vent line valve is quickly opened by manually to discharge the air and decrease the pressure. After the venting, the vent valve is quickly closed by manually. This process is repeated for the pre-determined test time.

Fig. 2.7 shows the vent frequency and vent period for P=0.32 MPa. Vent frequency increases and vent period decreases with the noncondensable mass fraction. For a given noncondensable mass fraction, vent frequency increases with system pressure. For P=0.194 MPa, we can obtain the periodic vent data up to Wair = 3%. For P=0.39 MPa, the maximum obtainable Wair is obout 0.5% for the periodic vent mode. It means that for high system pressure, through flow condition can be easily obtained for small noncondensable gas fraction and continuous condensation mode is hardly obtained. For low system pressure, the noncondensable gas fraction range for the periodic vent mode is relatively wide and the continuous condensation mode can be easily obtained.

Fig. 2.8 shows the condensation HTC for the periodic venting mode and through flow mode. Condensation performance for the through flow mode shows slightly better results than the periodic vent mode at a same noncondensable gas mass fraction. However, the degree of the improvement is very small and within the measurement error. It should be also noted that the periodic vent mode data and through flow data can be joined smoothly at the maximum noncondensable gas fraction for the vent mode. This result suggests the possibility of combining all three PCCS operation modes into one universal condensation heat transfer model.

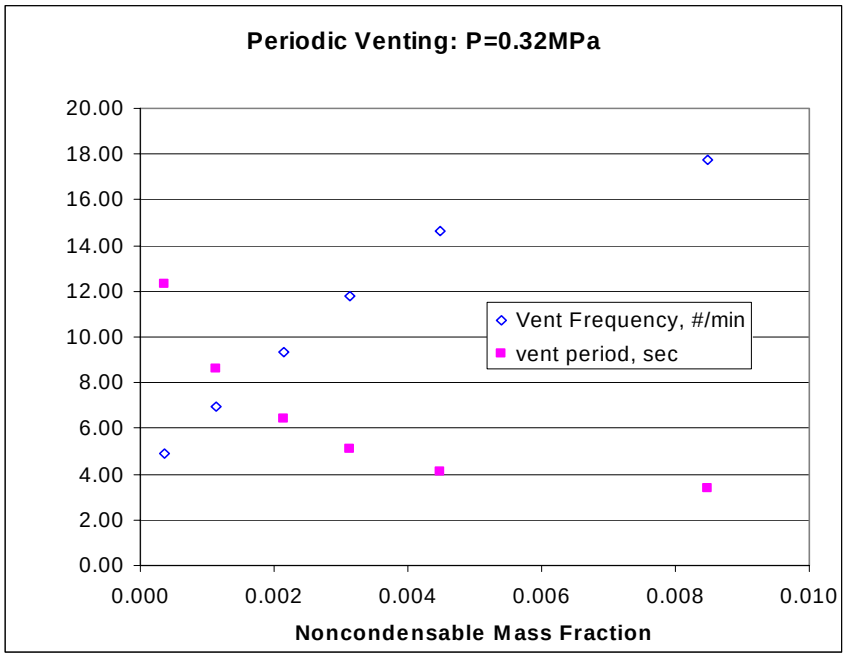

Figure 2.7 Vent Frequency and Vent Period for P=0.32MPa

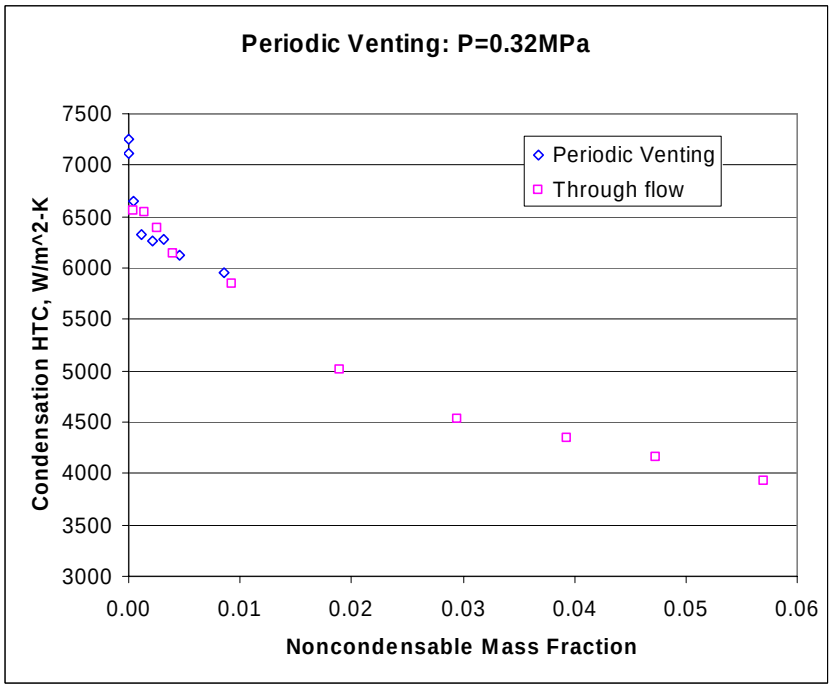

Figure 2.8 Condensation Heat Transfer Coefficients P=0.32MPa

4) Vent Analysis

If small amount of noncondensable gas is added at a steady state complete condensation mode, the pressure is increase. This increase in pressure comes from two sources. One is due to the addition of the noncondensable gas itself. Since it is not condensable, the gas is accumulated in the system and it makes one part of the pressure increase. The other is due to the addition of steam in the system caused by the degradation of the condensation. At a complete condensation condition, all steam is condensed. So there is no actual steam accumulation in the system. As small amount of the noncondensable gas is added in the system, the condensation performance is degraded, i.e., some amount of steam is not condensed. The uncondensed steam acts as a second source of system pressure increase.

In Ref. 3, the pressurization caused by the addition of the noncondensable gas is analyzed based on the ideal gas law.

3. ANALYTICAL MODELING

3.1 Boundary Layer Model with Self-Similar Velocity Profile Assumption

A boundary layer condensation model was developed for forced downflow of steam and non-condensable gas in vertical tube based on the self-similar velocity profile assumption. First the model was tested for pure steam condensation and the predicted heat transfer results were compared with the experimental data. Then the model was tested for condensation in the presence of non-condensable gas, air, and results of the predictions were compared to the published experimental data. The agreement was fairly good. Results are presented in Ref. 1.

3.2 Simple Pure Steam Model

For pure steam case, the condensation model was developed to see the effects of the various turbulent models and the interfacial shear stress models. In this analysis, two types of solution methods were obtained. In the first type, which is referred as Iteration method the vapor and liquid momentum equations are solved together with the different turbulent models for the gas region. In the second type the liquid momentum equation is solved and the appropriate interfacial shear stress model is used.

Fig. 3.1 shows the comparison between Kuhn's experimental data (Ref. 4) run 1.1-1 and analysis model. This case is inlet steam flow rate of 60.2 kg/hr, system pressure of 113.9 kPa. The local condensation heat transfer coefficients presented in Fig. 3.1 show very good agreement between test data and analysis. Fig. 3.2 shows the local condensation heat transfer coefficients for test run 1.1-4R1. Inlet steam flow rate(kg/hr)/pressure(kPa) conditions of test run 1.1-4R1 are 60.7/408.1. Detail Results are presented in Ref. 2.

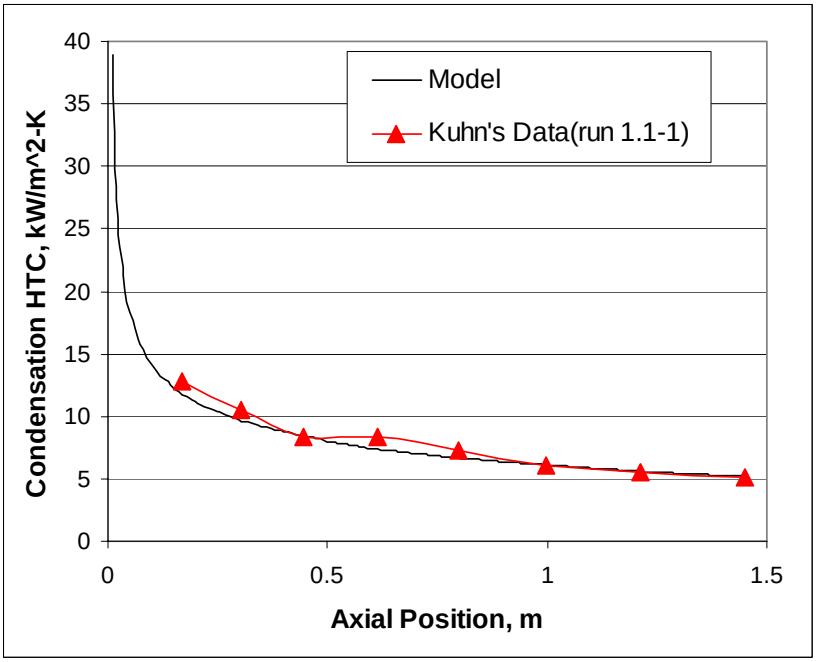

Figure 3.1 Condensation HTC Comparison with Kuhn's Data (run 1.1-1)

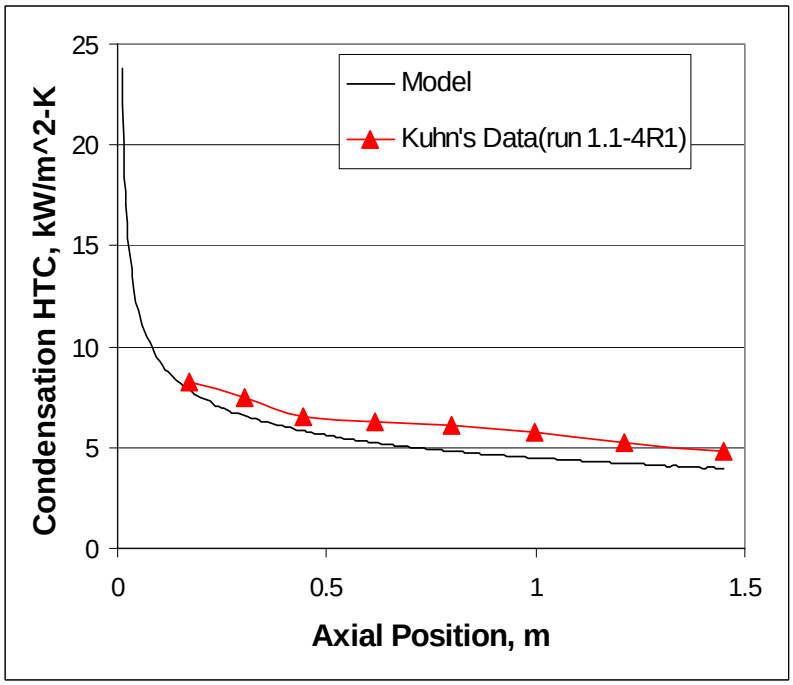

Figure 3.2 Condensation HTC Comparison with Kuhn's Data (run 1.1-4R1)

3.3 Boundary Layer Model

The analytic model described in the previous section is based on the self-similar velocity profile assumption. This assumption can be considered as a reasonable one for the engineering purpose.

But it may introduce some errors in the entrance region since the entrance region is the developing region of velocity, temperature, and noncondensable fraction. Also, the condensation at the entrance region is most efficient in the condenser tube. So, it is valuable to develop the new model without the self-similar assumption. For this purpose, the full boundary layer model was developed.

Figs. 3.3 ~ 3.7 show the comparison of HTC between this analysis model, Kuhn's data and model (Ref.4), Siddique's model (Ref. 5), and Vierow & Schrock model (Ref. 6). Table 3.1 summarized the analysis conditions. Next sections summarized the condensation models proposed by Siddique, Vierow & Schrock, and Kuhn.

1) Siddique's Condensation Correlation (Ref. 5)

$$Nu_G = 6.123 \cdot \mathrm{Re}_G^{0.223} \left(\frac{W_I - W_{bulk}}{W_I} \right)^{1.144} Ja^{-1.253}$$

where, $Ja = \dfrac{Cp_G \left(T_{bulk} - T_W \right)}{h_{fg}}$

$$\mathrm{Re}_G = \frac{\rho_G V d}{\mu_G}$$

$$Nu_G = \frac{h_{cond} \cdot d}{k_G}$$

$h_{cond} = \dfrac{q_I}{\left(T_{bulk} - T_W \right)}$: condensation heat transfer coefficient

$$T_{bulk} = T_{SAT}(P_{v,bulk})$$

$$\frac{P_{v,bulk}}{P_{TOT}} = \frac{1 - W_{bulk}}{1 - W_{bulk} \left(1 - \dfrac{M_v}{M_a} \right)}$$

$$W_{bulk} = \frac{m_a}{m_a + m_v}$$

2) Vierow & Shrock (UCB) Correlation (Ref. 6)

$$h_{UCB} = h_{Nu} \cdot f_1 \cdot f_2$$

where, $f_1 = \min(2 \quad , \quad 1 + 2.88E - 05 \cdot \mathrm{Re}_G^{1.18})$

$$f_2 = \begin{cases} 1 - 10 \cdot W_{bulk}^{\ 1.0} & for \quad W_{bulk} < 0.063 \\ 1 - 0.938 \cdot W_{bulk}^{\ 0.13} & for \quad 0.063 \le W_{bulk} < 0.6 \\ 1 - 1 \cdot W_{bulk}^{\ 0.22} & for \quad 0.6 \le W_{bulk} \end{cases}$$

$h_{Nu} = \dfrac{\delta_{Nu}}{k_L}$; Nusselt's condensation HTC

$$\delta_{Nu} = \left(\frac{3\mu_L \Gamma}{g\rho_L(\rho_L - \rho_G)} \right)^{1/3}$$; Nusselt's film thickness

3) Kuhn's Correlation (Ref. 4)

$$h_{KUHN} = h_{Nu} \cdot f_1 \cdot f_2$$

where, $f_1 = f_{1,SHEAR} \cdot f_{1,OTHER}$

$$f_{1,SHEAR} = \frac{\delta_{Nu}}{\delta_{SHEAR}}$$

δ_{SHEAR} = film thickness considering the interfacial shear

$$f_{1,OTHER} = 1 + 7.32E - 4 \cdot \left(\mathrm{Re}_f / 4 \right)$$

$$f_2 = \begin{cases} 1 - 2.601 \cdot W_{bulk}^{\ 0.708} & for \quad W_{bulk} < 0.1 \\ 1 - W_{bulk}^{\ 0.292} & for \quad 0.1 \le W_{bulk} \end{cases}$$

Table 3.1 Summary of Sample Run (47.5mm ID, 2.1m length tube)

Kuhn's Run #	Inlet Steam Flow, kg/hr	Inlet Air Flow, kg/hr	Inlet Pressure, Pa	Inlet Temp., C
533	61.9	0.602	402,500	146.6
513	29.6	0.314	408,500	142.7
535	60.7	3.19	403,500	141.0
517	29.7	5.78	404,600	127.0
355	59.6	35.34	492,600	140.8

From the comparison between the analysis, experiment data and various models, the followings are noted;

- Siddique's model can not predict well the entrance region. After entrance region, this model shows pretty good results.

- Vierow & Shrock model, Kuhn's model and boundary layer model show high condensation heat transfer coefficient at the entrance region. It is physically correct since the noncondensable

gas boundary layer thickness and the film thickness are thin and interfacial shear is big at the entrance region.

- Vierow & Shrock model predicts well only at the high inlet steam flow rate with high noncondensable gas fraction conditions. For low noncondensable gas fraction and small inlet steam flow conditions, this model overestimate the condensation heat transfer coefficients.

- Kuhn's model shows better results than the Vierow & Shrock model. But Kuhn's model still has considerable error especially at small inlet steam flow condition.

- Boundary layer model shows most appropriate results for all cases considered.

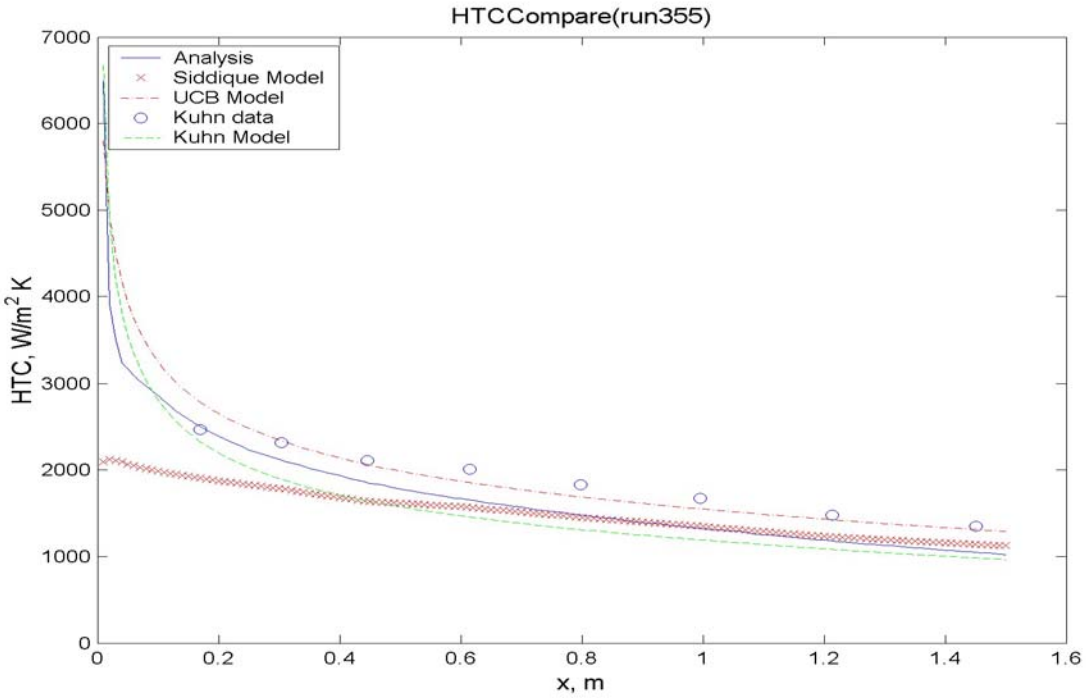

Figure 3.3 HTC Comparison : Kuhn's Run 355

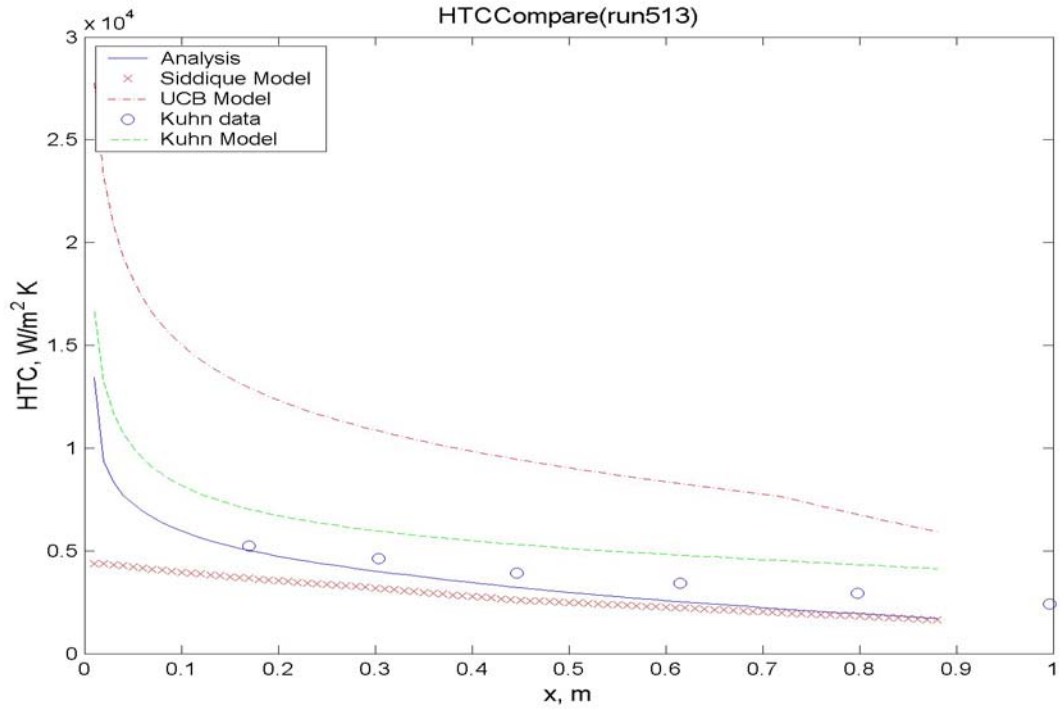

Figure 3.4 HTC Comparison : Kuhn's Run 513

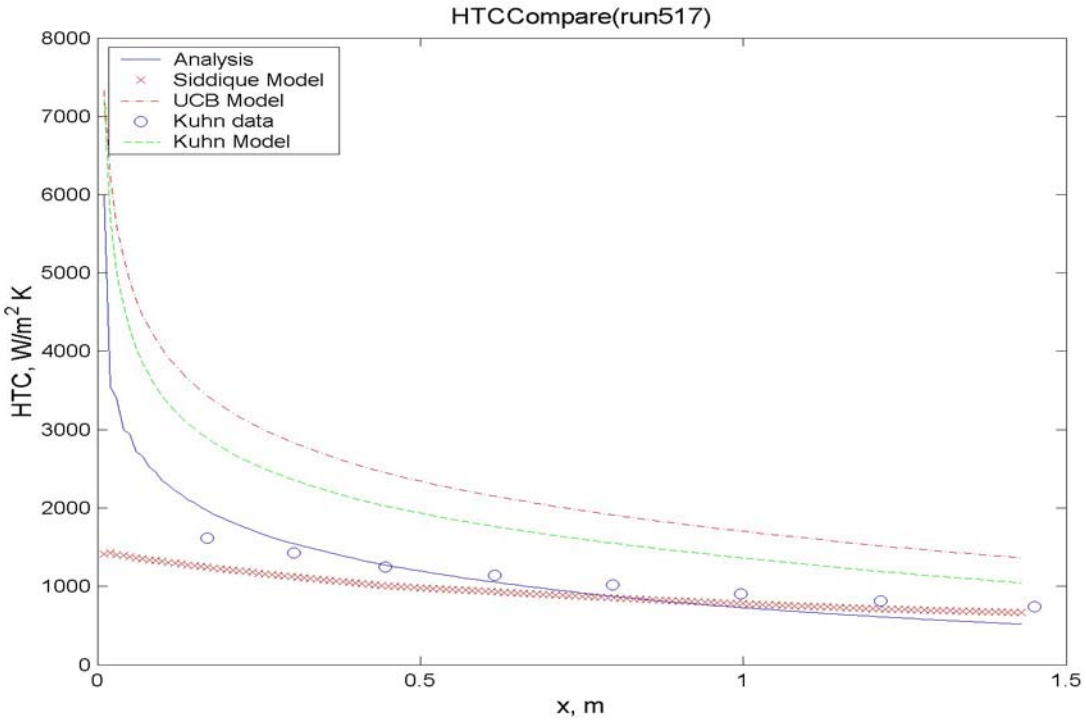

Figure 3.5 HTC Comparison : Kuhn's Run 517

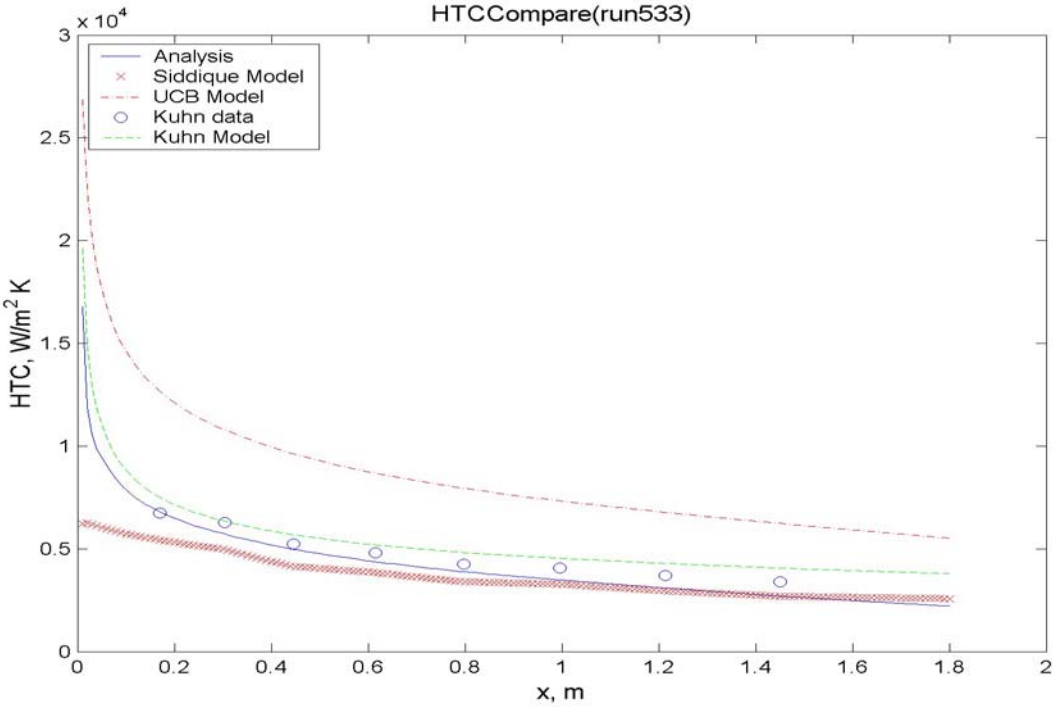

Figure 3.6 HTC Comparison : Kuhn's Run 533

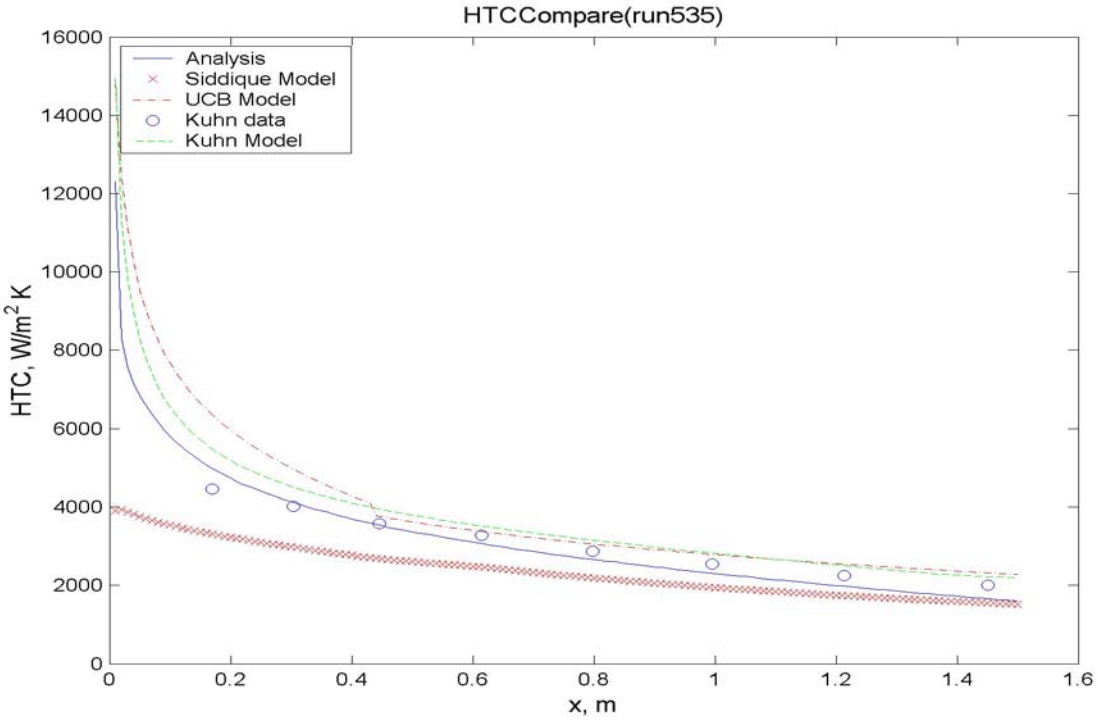

Figure 3.7 HTC Comparison : Kuhn's Run 535

4. ASSESSMENT OF RELAP5 CODE

Assessment of RELAP5 code against the experimental data is one of the main objectives of this research. For the assessment of RELAP5 code, we used the RELAP5/MOD3.3 beta version (Ref. 7). The RELAP5 computer code is a light water reactor transient analysis code developed for the U. S. Nuclear Regulatory Commission (NRC) for use in rulemaking, licensing audit calculations, evaluation of operator guidelines, and as a basis for a nuclear plant analyzer. RELAP5 is a highly generic code that, in addition to calculating the behavior of a reactor coolant system during a transient, can be used for simulation of a wide variety of hydraulic and thermal transients in both nuclear and nonnuclear systems involving mixture of steam, water, noncondensable, and solute.

RELAP5/MOD3.3 beta version has two wall film condensation models, the default and the alternative model. The default model uses the maximum of the Nusselt (laminar - Ref. 8) and Shah (turbulent - Ref. 9) correlations with a diffusion calculation (by Colburn-Hougen - Ref. 10) when noncondensable gases are present. The alternative model uses the Nusselt model with UCB (University of California at Berkeley) multipliers (Vierow and Schrock – Ref. 6), which is considering the effects of the noncondensable gases and the interfacial shear.

Using the RELAP5/MOD3.3 beta code, the experimental loop with secondary pool boiling section is simulated. For the assessment of RELAP5 code, experiment conditions are analyzed with the default and the UCB condensation model.

The RELAP5 nodalization of the experiment loop is shown in Fig. 4.1.

Complete Condensation Mode

For the comparison of the complete condensation mode, trip valve 808 is closed during the simulation. Results are shown in Figs. 4.2 ~ 4.6.

Fig. 4.2 shows the system pressure with the condensation rate. For a given condensation rate, the corresponding system pressure for the default model is very high. It means the default model underestimate the condensation rate. The discrepancy is much more severe at high condensation

rate. But for the UCB model, the pressure is very close to the test results although it is slightly higher.

Fig. 4.3 presents the same plot with Fig. 4.2 except change of the x- and y-axis. Fig. 4.4 shows the condensation heat transfer rate with system pressure. For a given system pressure, the condensation heat transfer rate for the default model is very low and it means the default model underestimate the condensation performance. However, the condensation heat transfer rate for the UCB model is very close to the test data although the condensation rate is slightly smaller than the test data. This difference is due to the facts that the total heat transfer rate from the condenser tube to the secondary pool, Q_{TOT} contains the condensation heat plus sensible heat transfer.

Fig. 4.5 presents the condensation HTC with system pressure. Default model shows small HTC but the trend is very similar to the test data. However, the condensation HTC from UCB model shows very small dependency with system pressure. This result can be more easily described with Fig. 4.6, inside wall temperature data. From Fig. 4.6, inside wall temperature for the default model is almost same with test data. It means the temperature difference between the saturation and inside wall is same between the test and default model. So the condensation HTC follows the trend of the condensation heat transfer rate. However, the inside wall temperature for the UCB model is higher than test data at high pressure condition. Then the temperature difference is smaller than test data. Since condensation rate is similar to the test data, the condensation HTC is higher than the test data at high pressure condition.

Through Flow Mode

For the comparison of the through flow mode with noncondensable gas, trip valve 808 is opened during the simulation. The representative case for the through flow mode, P=0.28 MPa and Msteam=3.6 g/s is selected and the results are shown in Figs. 4.7 ~ 4.10.

Fig. 4.7 shows the condensation rate with noncondensable gas mass fraction. Default model underestimate especially at the low gas fraction region. UCB model predict very well at low gas fraction region. But as gas fraction increases, the condensation rate decreases very rapidly comparing test data. Fig. 4.8 presents the condensation heat transfer rate with noncondensable gas mass fraction. This figure shows the similar trend with Fig. 4.7.

Condensation HTC is plotted in Fig. 4.9. This plot shows more evident trend of UCB model, which has large negative slope with gas fraction. This large slope can be explained by the inside wall temperature in Fig. 4.10.

From the previous comparison, the default model and the UCB model show quite different results. It must be also noted that the trends of the condensation rate and condensation heat transfer rate are also quite different with those of the condensation heat transfer coefficient. So, it can be concluded that we should compare the results comprehensively instead of comparing the heat transfer coefficients only. Generally, the UCB model shows better result than the default model as an aspect of the condensation rate and condensation heat transfer rate. However the trend of the condensation heat transfer coefficient for the UCB model shows large discrepancy with teat data for the complete condensation mode without noncondensable gas and through flow mode with noncondensable gas.

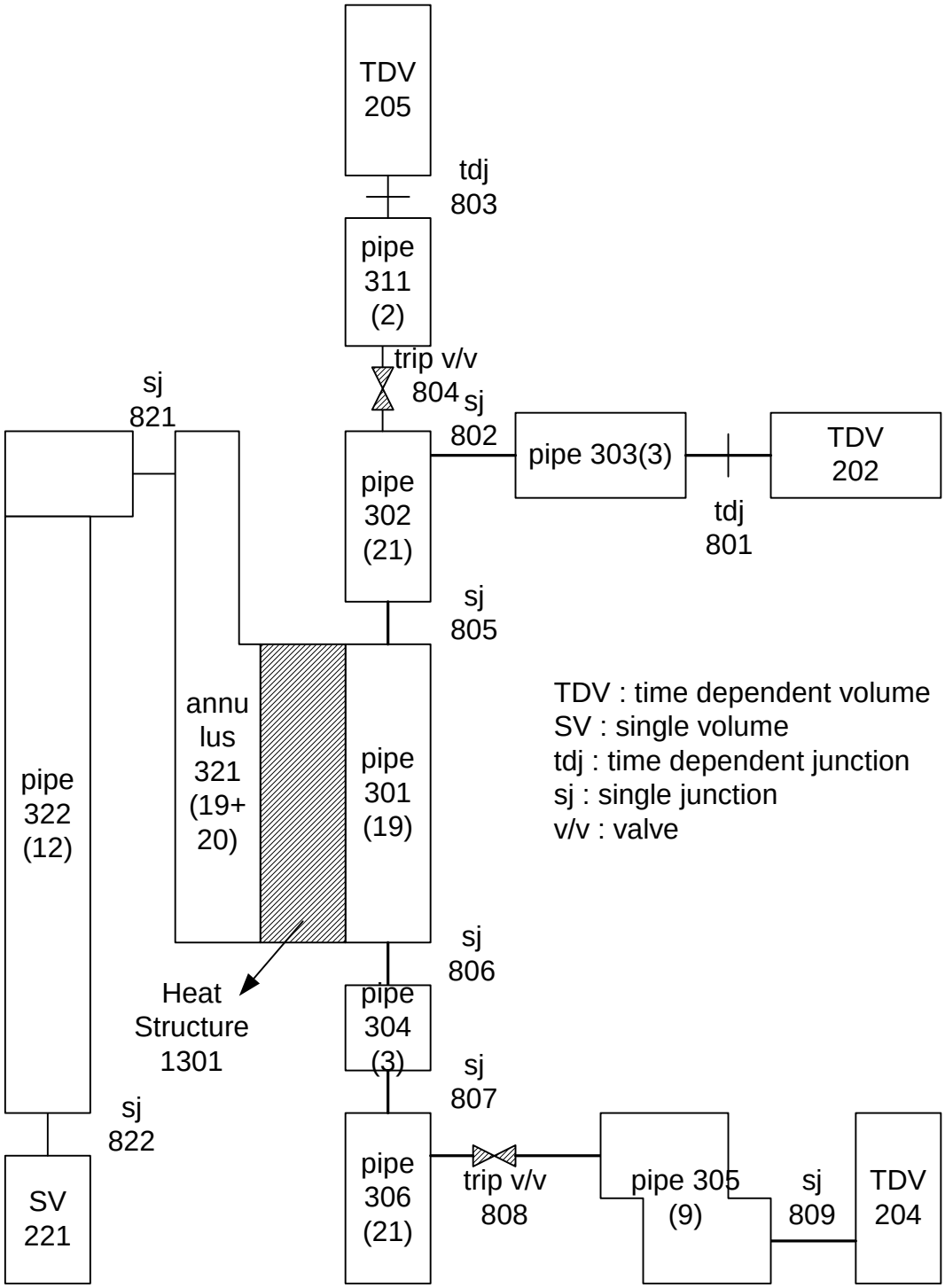

Figure 4.1 RELAP5 Nodalization

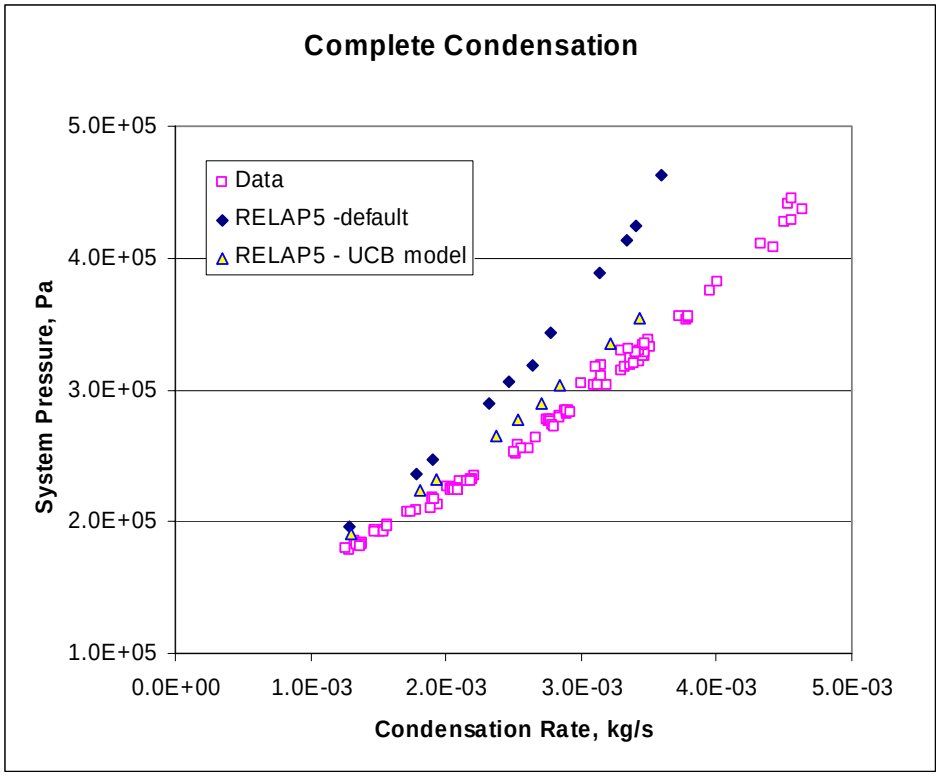

Figure 4.2 Comparison of System Pressure for Complete Condensation

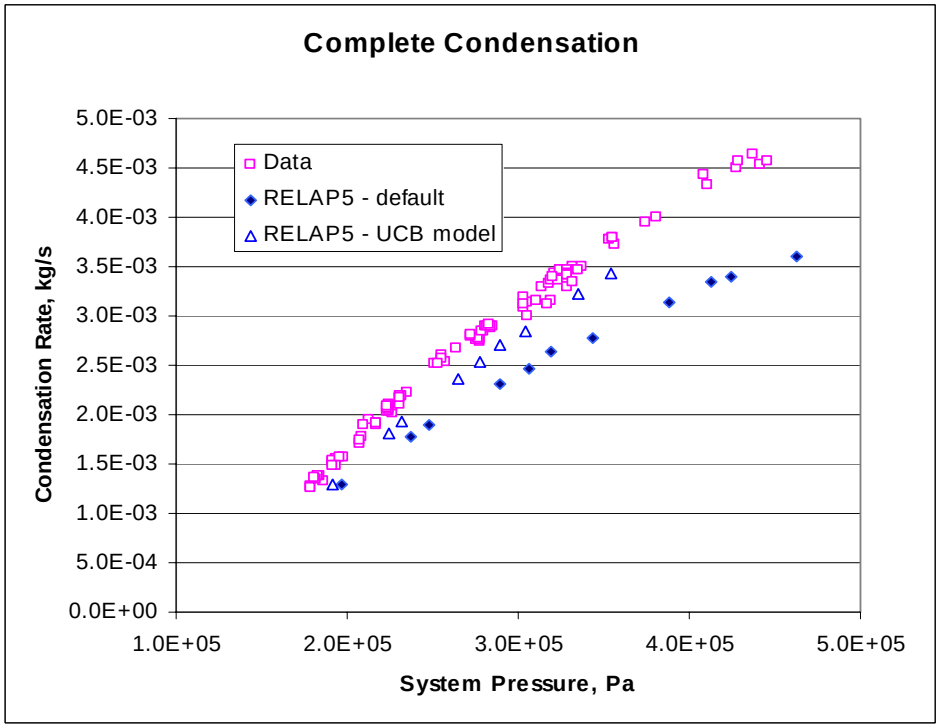

Figure 4.3 Comparison of Condensation Rate for Complete Condensation

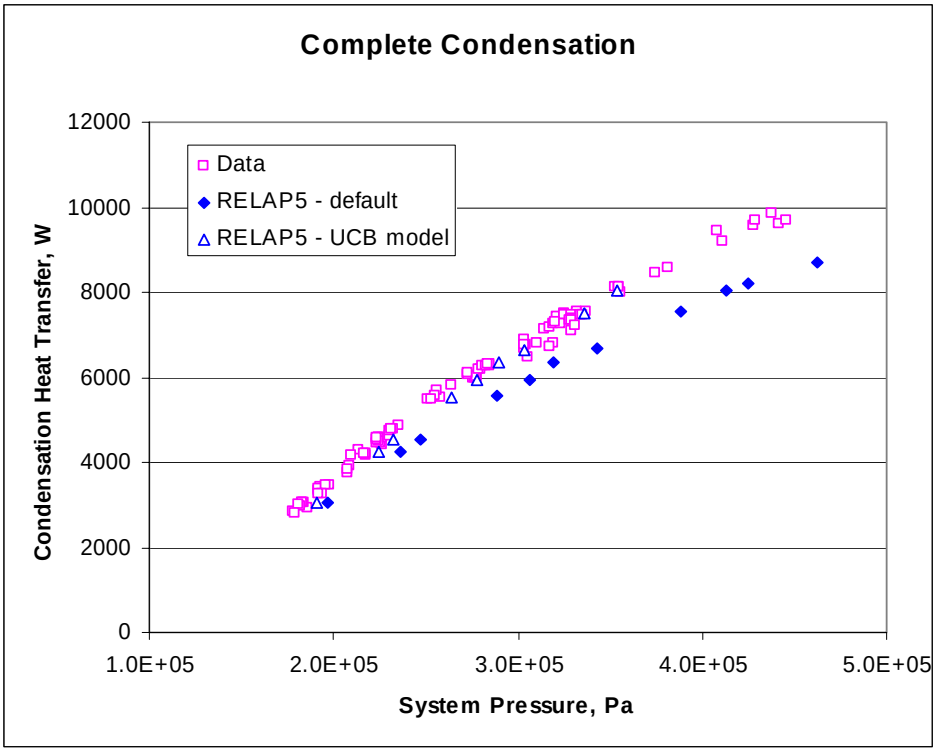

Figure 4.4 Comparison of Condensation Heat Transfer Rate for Complete Condensation

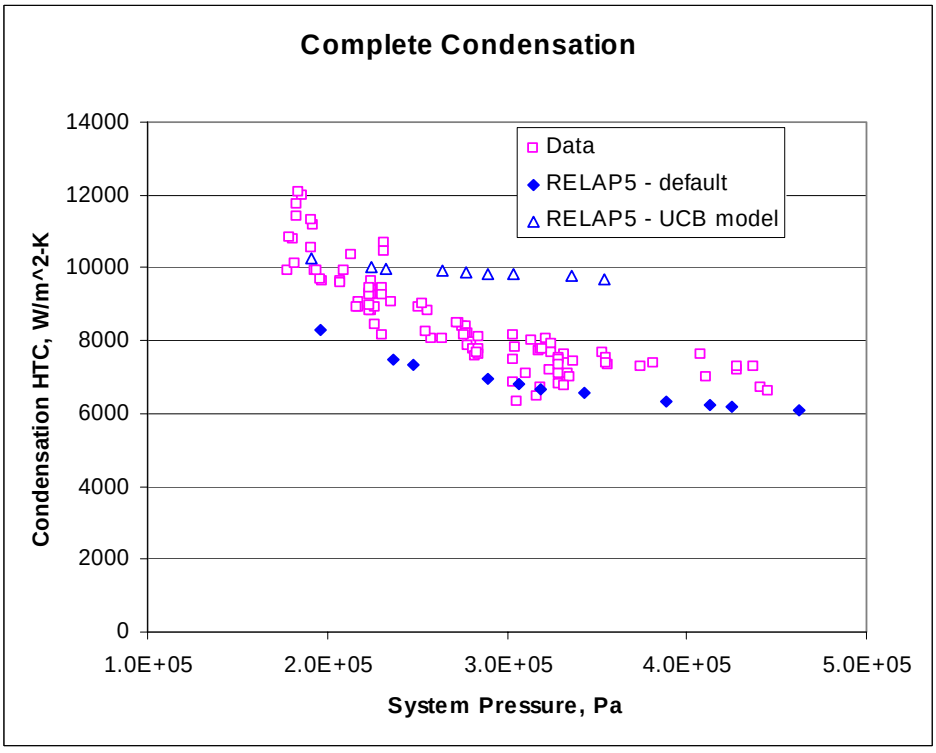

Figure 4.5 Comparison of Condensation HTC for Complete Condensation

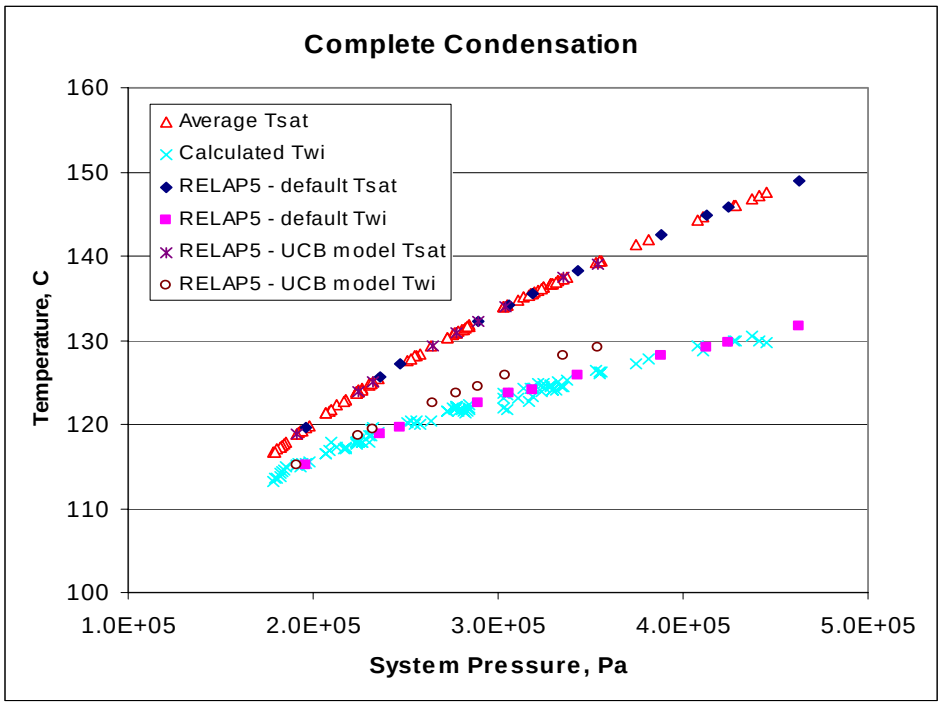

Figure 4.6 Comparison of Temperatures for Complete Condensation

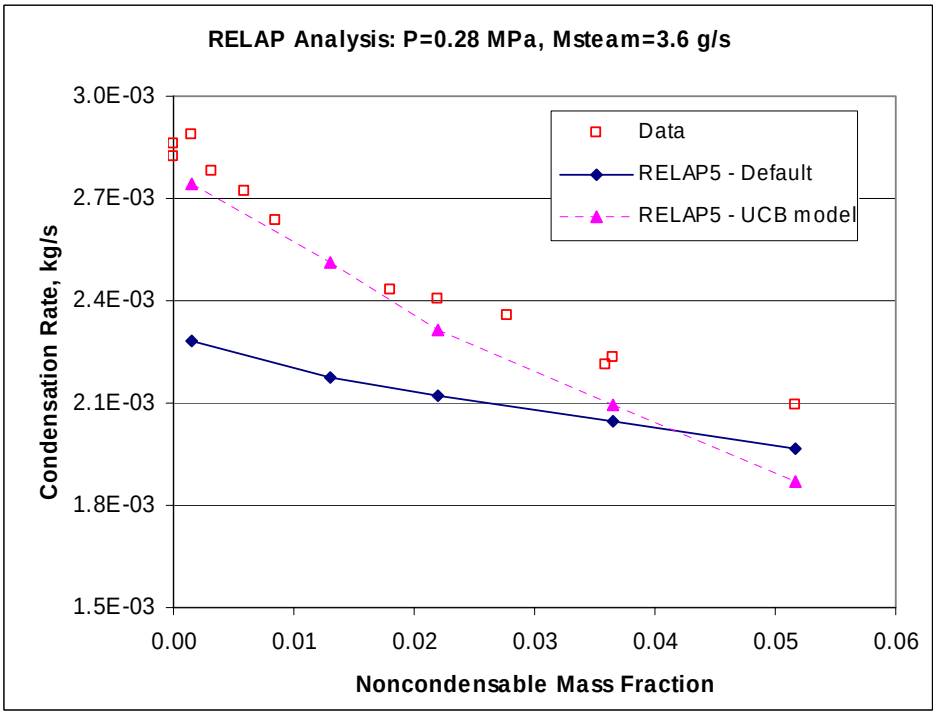

Figure 4.7 Comparison of Condensation Rate for Through Flow

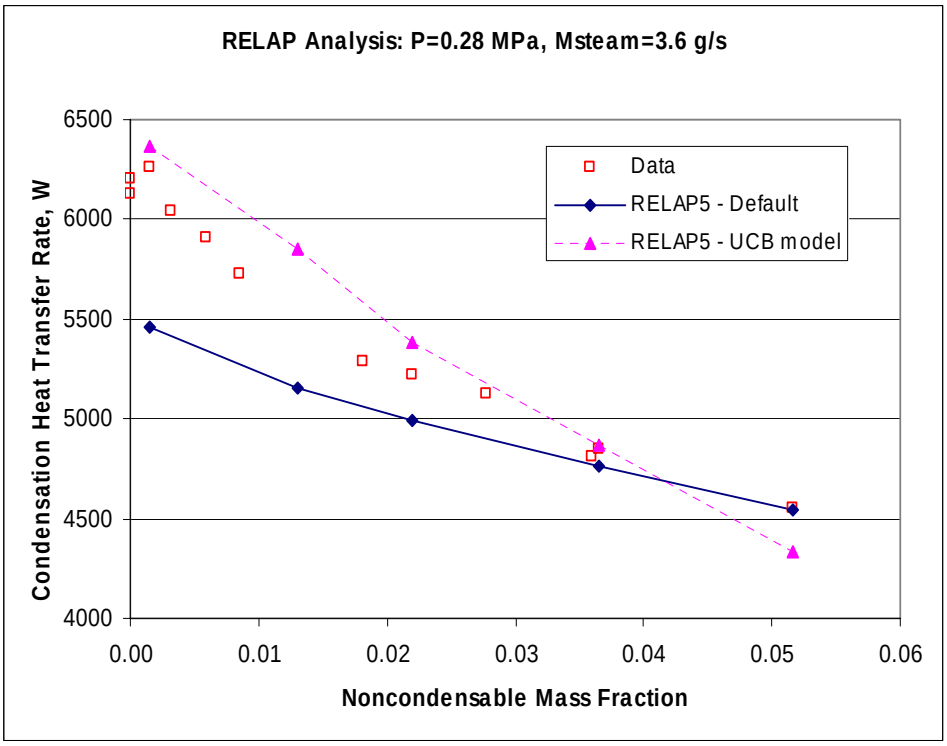

Figure 4.8 Comparison of Condensation Heat Transfer Rate for Through Flow

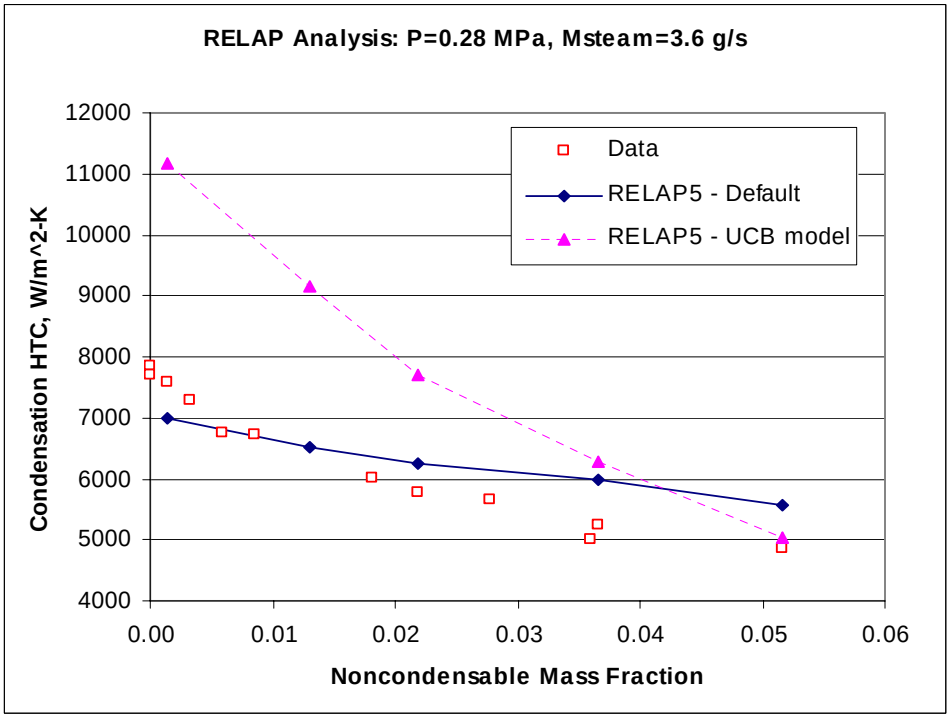

Figure 4.9 Comparison of Condensation HTC for Through Flow

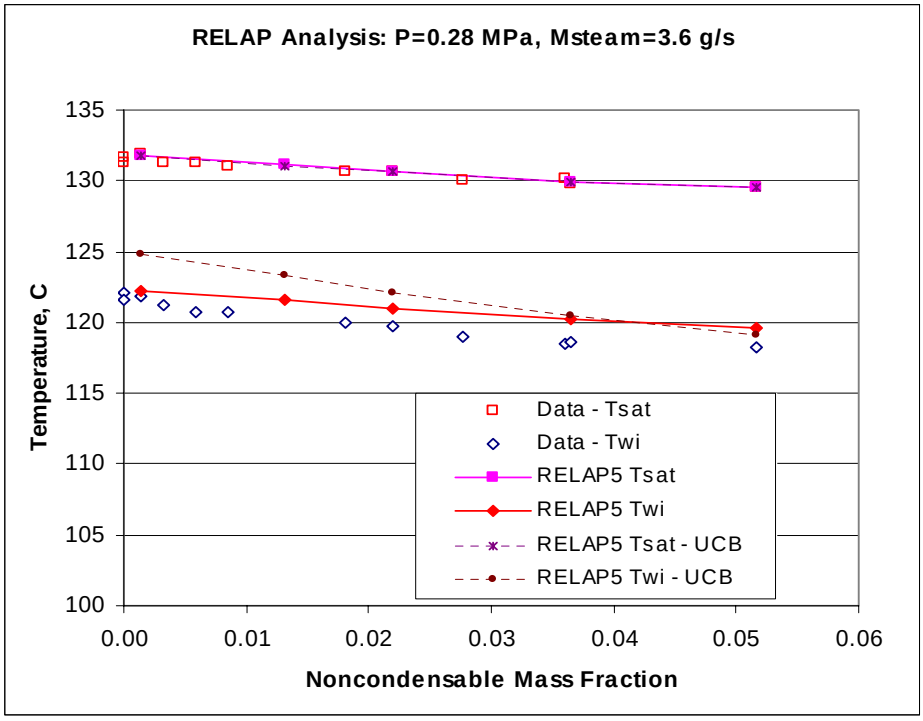

Figure 4.10 Comparison of Temperatures for Through Flow

References

1. S. T. Revankar, and D. Pollock, Analytical and Experimental Study of the Effects of Non-Condensable in a Passive Condenser System for the Advanced Boiling Water Reactor, PU/NE-01-3, May 2001.

2. S. T. Revankar, and S. Oh, Analytical and Experimental Study of the Effects of Non-Condensable in a Passive Condenser System for the Advanced Boiling Water Reactor, PU/NE-02-10, Sep. 2002.

3. S. T. Revankar, and S. Oh, Analytical and Experimental Study of the Effects of Non-Condensable in a Passive Condenser System for the Advanced Boiling Water Reactor, PU/NE-03-06, Jul. 2003.

4. Kuhn S. Z., Investigation of Heat Transfer from Condensing Steam-Gas Mixtures and Turbulent Films Flowing Downward inside a Vertical Tube, Ph. D. Thesis, Department of Nuclear Engineering, University of California at Berkeley, 1995.

5. Siddique M., The Effects if Non-Condensable Gaases in Condensation Under Forced Convection Conditions, PhD Thesis, MIT, 1990.
6. K.M. Vierow, V.E. Schrock, Condensation in a Natural Circulation Loop with Noncondensable Gases: Part I – Heat Transfer, Proc. of the Int. Conf. on Multiphase Flow, 183-186, 1991.
7. UREG/CR-5535/Rev 1, RELAP5/MOD3.3 Beta Code Manual, May 2001.
8. W.A. Nusselt , The Surface Condensation of Water Vapor, Ziesrhift Ver Deut. Ing., 60 pp. 541-546 & pp. 569-575, 1916.
9. M.M. Shah, A General Correlation for Heat Transfer During Film Condensation Inside Pipes, Int. J. Heat Mass Transfer Vol. 22, 547-556, 1979.
10. A.P. Colburn, O.A. Hougen, Design of Cooler Condensers for Mixture of Vapors with Non-condensable Gases, Industrial and Engineering Chemistry Vol. 26, 1178-1182, 1934.

Journal Papers Under Review

1. S. T. Revankar and S. Oh, Forced flow film condensation in a vertical tube with interfacial shear, International Journal of heat and Mass Transfer, 2002.
2. D. Pollock and S. T. Revankar. Analytical study of the effects of non-condensable gas in a forced flow vertical tube condenser, Journal of Heat Transfer, 2002.

Conference Papers

1. S. T. Revankar and D. Pollock, Effect Of Non-Condensable Gas In A Forced Flow Vertical Tube Condenser, Proceedings of NHTC'01, ASME 35th National Heat Transfer Conference, Anaheim, California, June 10-12, 2001.
2. S. T. Revankar and Seungmin Oh, Analytical and experimental study of noncondensable effect on passive condenser, to be presented at 2002 ANS Annual Meeting, Hollywood Florida, USA, June 9-13, 2002.

3. S. T. Revankar, Study of the effects of non-condensable in a passive condenser system for the advanced boiling water reactor, Twelfth International Heat Transfer Conference, Grenoble, France, August 18-23, 2002.
4. Seungmin Oh and S. T. Revankar, Effect Of Non-Condensable Gas On The Tube Condenser Operating In Passive Mode, 2003 ASME Summer Heat Transfer Conference, Las Vegas, Nevada, USA, July 21–23, 2003.
5. S. T. Revankar and Seungmin Oh, Investigation of the Non-Condensable Effect and the Operational Modes of the Passive Condenser System, to be presented at the Tenth International Topical Meeting on Nuclear Reactor Thermal Hydraulics, Seoul, Korea, October 5-11, 2003.